Doping Graphene

DOI: 10.1002/ange.201403382

Direct Observation of Atomic Dynamics and Silicon Doping at a Topological Defect in Graphene**

Zhiqing Yang, Lichang Yin, Jaekwang Lee, Wencai Ren, Hui-Ming Cheng, Hengqiang Ye, Sokrates T. Pantelides, Stephen J. Pennycook, and Matthew F. Chisholm**

Abstract: *Chemical decoration of defects is an effective way to functionalize graphene and to study mechanisms of their interaction with environment. We monitored dynamic atomic processes during the formation of a rotary Si trimer in monolayer graphene using an aberration-corrected scanning-transmission electron microscope. An incoming Si atom competed with and replaced a metastable C dimer next to a pair of Si substitutional atoms at a topological defect in graphene, producing a Si trimer. Other atomic events including removal of single C atoms, incorporation and relocation of a C dimer, reversible C−C bond rotation, and vibration of Si atoms occurred before the final formation of the Si trimer. Theoretical calculations indicate that it requires 2.0 eV to rotate the Si trimer. Our real-time results provide insight with atomic precision for reaction dynamics during chemical doping at defects in graphene, which have implications for defect nano-engineering of graphene.*

Pure graphene has limited practical applications due to its low carrier density, zero band gap, and chemical inertness. Local structures of graphene can be modified to obtain useful properties[1] and applications such as semiconductor nano-devices,[2] batteries,[3] and chemical separation.[4] Chemical treatment is one of the practical methods to functionalize graphene. The single-atom thickness nature of graphene makes it an ideal medium for revealing its own defect structure, bonding and dynamics on the atomic level.[5] The ability to directly observe reactions on the atomic level, which has long been expected in many areas of science and technology, can significantly advance our understanding on the physical and chemical mechanisms controlling the formation of functional structures.[5b,6] However, atom-by-atom, real-time monitoring of the chemical processes that produce heterogeneous structures remains challenging, even for the monolayer two-dimensional materials, including graphene,[6] although atom-by-atom structural characterization has been realized.[7] In this report, we demonstrate that annular dark-field (ADF) imaging using an aberration-corrected scanning transmission electron microscope (STEM) provides a feasible in-situ way to monitor the atomic sequence of Si-graphene reactions at topological defects and the dynamics of the resulting structures with all relevant atoms resolved and identified.

Graphene samples were reduced from graphene oxide.[8] Atomic-scale observations were performed using an aberration-corrected STEM operated at 60 kV, in order to reduce beam etching. A detector half-angle range of 58–200 mrad was used to record ADF images. This imaging setting, in combination with a double Gaussian filter to remove noise and probe tail effects in the high-resolution ADF images (Supporting Information (SI) Figure S1, S2), is able to realize atom-by-atom identification of all atoms in monolayer materials.[7] To obtain in-depth understanding of mechanisms controlling the formation of the observed structures, as well as their dynamical behaviors, first-principles calculations based on density functional theory,[9] were performed.

Figure 1 and Supporting Movie S1 show the atomic structures of a complex topological defect with two heavier substitutional atoms in monolayer graphene and the structure's dynamic evolution. The heavier atoms are determined to be Si based on intensity quantification and electron energy-loss spectroscopy measurements (SI Figure S2, S3).[10] Silicon impurities were likely introduced from the glassware used to process the graphene.[11] The STEM-ADF image in Figure 1 a shows two silicon atoms, Si_1 and Si_2 in substitutional sites in a 555–777 complex defect consisting of three dislocations (each of which is a paired pentagon and heptagon ring of atoms[6b,12]). After 24 s of observation, the carbon atom labeled C_1 was removed due to knock-on damage, and the configuration relaxed to the 555–666 structure shown in

[*] Dr. Z. Q. Yang, Dr. L. C. Yin, Dr. W. C. Ren, Prof. H.-M. Cheng, Prof. H. Q. Ye
Shenyang National Laboratory for Materials Science
Institute of Metal Research, Chinese Academy of Sciences
72 Wenhua Rd, Shenyang 110016 (China)
E-mail: yangzq@imr.ac.cn
Dr. J. Lee, Dr. M. F. Chisholm
Division of Materials Science and Technology
Oak Ridge National Laboratory
Oak Ridge, TN 37831 (USA)
E-mail: chisholmmf@ornl.gov
Prof. S. T. Pantelides
Department of Physics and Astronomy, Vanderbilt University
Nashville, TN 37235 (USA)
Prof. S. J. Pennycook, Dr. M. F. Chisholm
Department of Materials Science and Engineering
University of Tennessee
Knoxville, TN 37996 (USA)

[**] Z.Q.Y. and M.F.C. conceived the study. Z.Q.Y. performed experiments and wrote the manuscript. J.L. and L.C.Y. performed density functional calculations. W.C.R. and H.M.C. prepared graphene samples. This research was supported by the U.S. Department of Energy, Basic Energy Science, Materials Science and Engineering Division, a ShaRE User program sponsored by DOE-BES, NSF of China (51171189, 51172240, 51221264, 51290273, 51371178, 51390473, 51325205), MoST 2012AA030303, and CAS (KGZD-EW-303-1, Shenyang Supercomputing Center).

Supporting information for this article is available on the WWW under http://dx.doi.org/10.1002/anie.201403382.

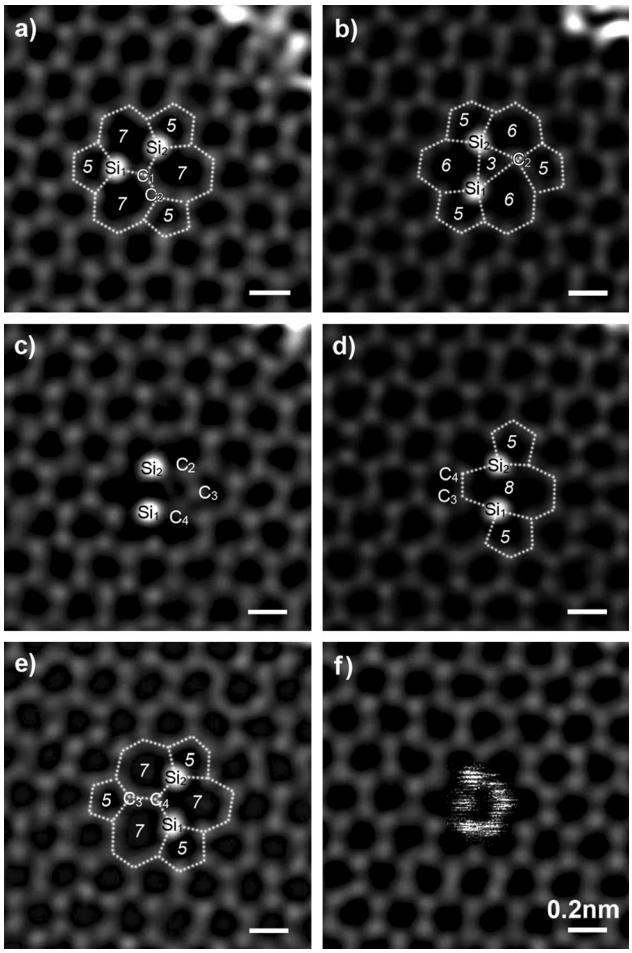

Figure 1. Lattice dynamics during the formation of a Si trimer in monolayer graphene. a) $t = 0$ s, a 555–777 defect with two Si substitutional atoms. b) Rotation of the Si dimer after losing a carbon atom at $t = 24$ s. c) Incoming of a carbon dimer at $t = 62$ s. d) Loss of one carbon atom and relocation of a carbon dimer at $t = 69$ s. e) Reversible bond rotation of the relocated carbon dimer to (d) in the next ca. 20 min. f) Atomic vibration upon the incoming of a third Si atom at $t \approx 24$ min. The extremely bright intensity peaks at the upper right corner in (a) and (b) are due to adsorption of Si atoms on graphene. The silicon atoms shown in panel (f) were excluded from image filtering, in order to reserve the streaks produced by the jumping of Si atoms (a corresponding unfiltered image is given in SI Figure S4). In (f), it is extremely hard to extract information for carbon atoms C_3 and C_4 that interact with the Si atoms dynamically, due to the high intensities from the moving Si atoms. Dotted lines outline the characteristic structures, 555–777, 555–666 and 5–8–5.

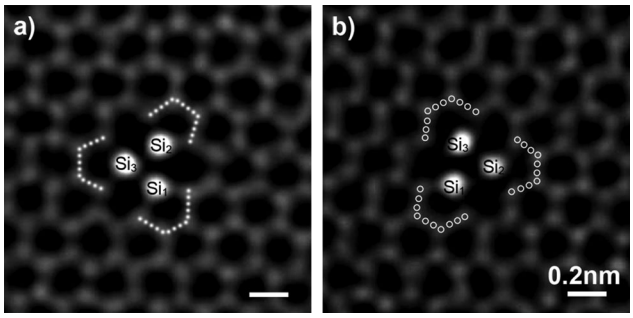

Figure 2. Rotation of the Si trimer. a) $t = 0$ s. b) $t = 67$ s. White dots and circles outline the armchairs which support the Si trimer. The Si trimer moves from one set (panel a, dot) to the other set (panel b, circle) of armchairs through a rotation by 60°. One of the silicon atoms is in the graphene plane, according to first-principles calculations as shown in Figure 3 c.

Figure 1 b, through a counterclockwise 60° rotation of the triangle of C_2-Si_1-Si_2 around its center. At some point a carbon dimer (C_3 and C_4) was incorporated into the relatively larger opening to the right of the Si atoms with the C_3–C_4 bond inclined, as demonstrated by the shorter C_3–C_4 distance of about 1.1 Å (i.e. 0.3 Å less than C–C bonds in graphene) measured in Figure 1 c. The C_3–C_4 dimer could not stay at the original incorporated position, and it was quickly relocated to the left side of the two Si atoms, forming a 5–8–5 configuration, as shown in Figure 1 d. The relocation of the C_3–C_4 dimer pushed the two Si atoms rightwards. In addition, atom C_2 was lost accompanying the C_3–C_4 relocation. Dynamically reversible transformations between the 5–8–5 and 555–777 structures then continued for about 22 min through 90° bond rotation of C_3–C_4 (Figure 1 d,e).

The incoming of another Si atom disturbed the C–C bond rotation, and induced further structural modification at the topological defect, as shown in Figure 1 f. The horizontal streaks in Figure 1 f indicate that this third silicon atom was attracted to the defect and hovered in the area for some time until it was finally incorporated into the underlying structure to form a silicon trimer (Figure 2). Those bright streaks were produced when the atom stayed at a given position for a period longer than that for the scanning electron beam to pass the atom. If the Si atom jumped away once the scanning electron beam arrived, black streaks would appear on the ADF image. Atoms Si_1 and Si_2 also kept on moving back and forth in the horizontal direction when the third silicon atom was hovering. The third Si atom was not knocked away by the incident scanning electrons, which can be attributed to the strong attraction between the silicon atom and the topological defect (SI Figure S5).[5b] The attraction potential not only reduces the jump distance of the activated Si atom, but also can pull it back quickly to the topological defect, if it is not deviated too far by the scanning electron beam.

The maximum energy that a 60 keV electron can transfer to a carbon atom is 11.6 eV.[13] This energy is below the mean displacement energy of 14.1 eV for edge carbon atoms,[14] but above the calculated energy of 3.9 eV for C_3–C_4 bond rotation.[6b] Therefore, the energy transferred from an incident electron is most likely to result in C_3–C_4 bond rotation, instead of removal of the dimer from the graphene. Whatever the mechanism is, the C_3–C_4 dimer appeared to be stable and kept rotating under the electron beam, until the arrival of the third silicon atom. First-principles calculations (SI Figure S6) show that substitution of a carbon atom by a silicon atom entails an energy increase of only 0.7 eV at the 555–777 defect. Therefore, one adsorbed Si atom in the vicinity would move toward the topological defect by the strong attraction energy between them (SI Figure S5), and subsequently replaced the less stable C_3–C_4 dimer. The third Si atom was not incorporated into the topological defect immediately upon its arrival (Figure 1 f), which is most likely that there was not enough

place when the C_3–C_4 dimer was still there. The replacement was probably assisted by energy transfer from the incident fast electrons.

The resulting silicon trimer continues to rotate by 60° or multiples of 60°, while the surrounding carbon atoms remain in their lattice sites, as shown in Figure 2 and Supporting Movie S2. The two structures shown in Figure 2 are energetically equivalent (degenerate) with six-fold rotational symmetry. This Si trimer-graphene system is very robust, since no knock-on damage occurred under the intense electron beam for an observation period of over 12 min. The long lifetime of the silicon trimer under the 60 kV electron beam is in stark contrast to the high mobility of other defects in pristine graphene.[5c,12a] The silicon trimer shown in Figure 2 can also be similarly created by removing a hexagonal ring of carbon atoms from a graphene layer,[7,14] then filling the pore with three silicon atoms. It can be expected that controlled replacement of carbon atoms by Si atoms may produce in-plane dots, wires, or arrays that can be used to fabricate useful nanostructures or nanodevices based on a graphene membrane.

The fully relaxed structures for the complex with a carbon dimer parallel and perpendicular to a silicon dimer (Figure 1 d,e) are shown in Figure 3 a and b, respectively. The carbon dimer is displaced out of the graphene plane, while the silicon dimer remains basically in the graphene plane in both cases. The 90° rotation of the carbon dimer results in the transformation of a 5–8–5 defect structure (Figure 1 d and 3 a) to a 555–777 configuration (Figure 1 e and 3 b), increasing the distance between the two silicon atoms by 0.1 Å, which is consistent with experimental observations. In the case of the silicon trimer, one silicon atom (Si_2) remains basically in the graphene plane, while the other two (Si_1 and Si_3) stay about 0.9 Å out of the graphene layer on opposite sides of the graphene layer, as shown in Figure 3 c. First-principles calculations also show that the silicon trimer practically does not move perpendicular to the graphene layer during the rotation (SI Figure S7). The deviation of atoms Si_1 and Si_3 from the graphene layer is attributed to their preferred sp^3 hybridization (SI Figure S8).

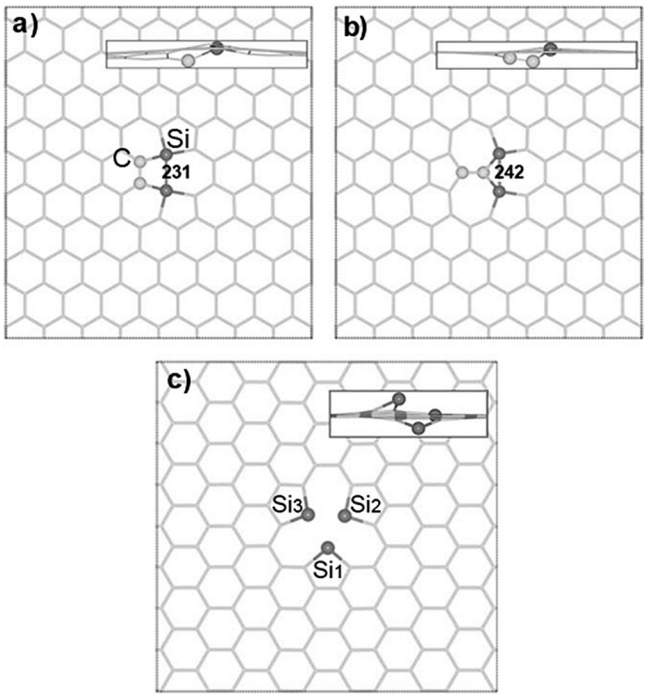

Figure 3. Calculated three-dimensional structures for monolayer graphene with Si atoms. a) 5–8–5 defect with a Si dimer. b) 555–777 defect with a Si dimer. c) Si trimer. Numbers in panels (a) and (b) indicate the corresponding Si–Si bond lengths in picometers. Insets are the corresponding local side views of the defect structures.

The binding energy of Si atoms in the trimer to graphene is calculated to be about 8.8 eV which is much higher than the maximum energy of about 5.0 eV that can be transferred from 60 keV electrons to a silicon atom.[13] Therefore, the Si trimer structure is durable under the electron beam. The energy barrier to rotate the silicon trimer was calculated to be about 2.0 eV (Figure 4 e) using the nudged elastic band method,[9e] which corresponds to a tangential force of 4.3 nN parallel to the graphene layer pushing the silicon trimer to do a stepwise rotation of 60° (Figure 4 a–d) in about 140 femtoseconds (Supporting Information).[15] The energy (2.0 eV) required to rotate the Si trimer is even much lower than that (3.9 eV) to rotate the C_3–C_4 dimer shown in Figure 1 d and e, while whole carbon hexagonal rings in graphene are practically non-rotatable. Therefore, replacing a carbon hexagonal ring with a silicon trimer has produced a terahertz (10^{12} Hz) rotary structure with relatively low friction in graphene. During our STEM observations, the electron beam can transfer kinetic energy to any silicon atom in the trapped trimer and make it move. This generates a torque on the trimer that results in rotation. The observed dynamic behavior of the Si trimer under the scanning electron beam is more or less similar to the current-driven rotation of molecules under the tip of a scanning tunnelling microscope.[16] The rotary silicon trimer may have potential applications in bridging media separated by the impermeable graphene membrane. A previous paper reported transition of a Si_6 cluster trapped in a graphene pore between two structures with different energy due to the jumping of one Si atom between two positions, while the other five Si atoms kept stationary.[17] The rotation of the whole Si trimer as a result of cooperative movement of all three atoms is different from the structural transition of a Si_6 cluster produced by the oscillatory motion of only one silicon atom.

It has been demonstrated that doping can modify the electronic structure and catalytic behavior of graphene.[18] For example, first-principles calculations showed that doping single Si atoms in graphene could reduce the dissociation barrier of O_2 from 3.18 eV to 0.21 eV.[18b] Our experimental results on the atomic structure and dynamic behavior of Si dopants at topological defects in graphene may have implications for better understanding and modeling of catalytic behavior of doped graphene. Furthermore, grafting or growing other nanomaterials, like a carbon nanotube (CNT), to an embedded dopant cluster would produce a graphene–dopant–CNT hybrid nanostructure.[6a]

In summary, we have demonstrated that in-situ aberration-corrected STEM enables atomic level monitoring of critical steps in the process of forming a rotary Si trimer

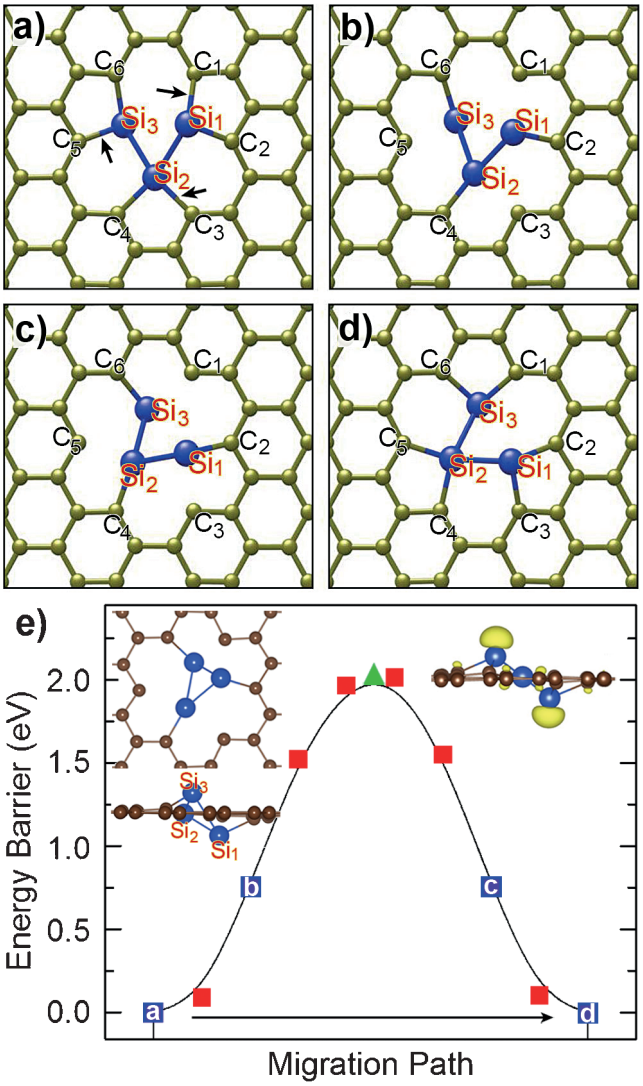

Figure 4. First-principles calculations on the rotation of the Si trimer embedded in monolayer graphene. a–d) Four relaxed atomic structures during a clockwise 60° rotation of the silicon trimer. e) Calculated energy barrier for rotating the trimer by 60° with an inset (upper left) showing the top and side views of atomic structure at a rotation angle of 30° (indicated by a green triangle), and an inset (upper right) showing the distribution of P_z partial electrons (yellow) for atoms at the defect shown in panel (a) (see SI Figure S8 and S9 for details on the electronic structure). Si atoms are shown in blue. Atom Si_2 is in the graphene plane. There are six equivalent orientations for the Si trimer to fit in with the graphene pore. Letters "a"–"d" and blue squares in panel (e) indicate the corresponding states shown in panels (a)–(d). All the silicon atoms make bonds with two carbon atoms when they are at the armchair position. Only one of the two Si–C bonds for each Si atom is broken, as indicated by arrows in panel (a), to facilitate the rotation. Additionally, atoms Si_1 and Si_3 keep bonded to atom Si_2 during the rotation. At the transition state with a rotation angle of 30°, all the three Si atoms bonded to each other, as shown by the inset at the upper left corner in (e).

through Si–graphene reactions at a topological defect in a graphene monolayer. Our real-time observations shed light on understanding of chemical reactions to functionalize graphene and other two-dimensional materials on the atomic level. The experimental observations on the incorporation and relocation of a C dimer, and the dynamic jump of the adsorbed Si atom before it was incorporated into the topological defect provide direct evidence on dynamic interactions between dopant atoms and defects with high reactivity in graphene, which may be common in other two-dimensional materials or surfaces of bulk materials. Problems of surface chemistry are expected to be greatly helped by the ability to see where and how a single foreign atom interacts with the surface.

Received: March 16, 2014
Published online: June 30, 2014

Keywords: density functional calculations · doping · electron microscopy · graphene · silicon

[1] a) M. T. Lusk, L. D. Carr, *Phys. Rev. Lett.* **2008**, *100*, 175503; b) D. C. Elias, R. R. Nair, T. M. G. Mohiuddin, S. V. Morozov, P. Blake, M. P. Halsall, A. C. Ferrari, D. W. Boukhvalov, M. I. Katsnelson, A. K. Geim, K. S. Novoselov, *Science* **2009**, *323*, 610–613; c) R. R. Nair, M. Sepioni, I. L. Tsai, O. Lehtinen, J. Keinonen, A. V. Krasheninnikov, T. Thomson, A. K. Geim, I. V. Grigorieva, *Nat. Phys.* **2012**, *8*, 199–202; d) J. Lahiri, Y. Lin, P. Bozkurt, I. I. Oleynik, M. Batzill, *Nat. Nanotechnol.* **2010**, *5*, 326–329; e) S. Kattel, P. Atanassov, B. Kiefer, *J. Phys. Chem. C* **2012**, *116*, 8161–8166.

[2] a) K. S. Novoselov, V. I. Fal'ko, L. Colombo, P. R. Gellert, M. G. Schwab, K. Kim, *Nature* **2012**, *490*, 192–200; b) K. Kim, J. Y. Choi, T. Kim, S. H. Cho, H. J. Chung, *Nature* **2011**, *479*, 338–344; c) K. S. Novoselov, A. K. Geim, S. V. Morozov, D. Jiang, Y. Zhang, S. V. Dubonos, I. V. Grigorieva, A. A. Firsov, *Science* **2004**, *306*, 666–669; d) Y. M. Lin, A. Valdes-Garcia, S. J. Han, D. B. Farmer, I. Meric, Y. Sun, Y. Wu, C. Dimitrakopoulos, A. Grill, P. Avouris, K. A. Jenkins, *Science* **2011**, *332*, 1294–1297.

[3] N. Li, Z. P. Chen, W. C. Ren, F. Li, H. M. Cheng, *Proc. Natl. Acad. Sci. USA* **2012**, *109*, 17360–17365.

[4] a) V. Berry, *Carbon* **2013**, *62*, 1–10; b) J. S. Bunch, S. S. Verbridge, J. S. Alden, A. M. van der Zande, J. M. Parpia, H. G. Craighead, P. L. McEuen, *Nano Lett.* **2008**, *8*, 2458–2462; c) H. W. Kim, H. W. Yoon, S. M. Yoon, B. M. Yoo, B. K. Ahn, Y. H. Cho, H. J. Shin, H. Yang, U. Paik, S. Kwon, J. Y. Choi, H. B. Park, *Science* **2013**, *342*, 91–95.

[5] a) J. H. Warner, E. R. Margine, M. Mukai, A. W. Robertson, F. Giustino, A. I. Kirkland, *Science* **2012**, *337*, 209–212; b) O. Cretu, A. V. Krasheninnikov, J. A. Rodriguez-Manzo, L. Sun, R. M. Nieminen, F. Banhart, *Phys. Rev. Lett.* **2010**, *105*, 196102; c) C. O. Girit, J. C. Meyer, R. Erni, M. D. Rossell, C. Kisielowski, L. Yang, C.-H. Park, M. F. Crommie, M. L. Cohen, S. G. Louie, A. Zettl, *Science* **2009**, *323*, 1705–1708; d) J. M. Yuk, J. Park, P. Ercius, K. Kim, D. J. Hellebusch, M. F. Crommie, J. Y. Lee, A. Zettl, A. P. Alivisatos, *Science* **2012**, *336*, 61–64.

[6] a) W. Gao, J. E. Mueller, J. Anton, Q. Jiang, T. Jacob, *Angew. Chem.* **2013**, *125*, 14487–14491; *Angew. Chem. Int. Ed.* **2013**, *52*, 14237–14241; b) G. D. Lee, C. Z. Wang, E. Yoon, N. M. Hwang, D. Y. Kim, K. M. Ho, *Phys. Rev. Lett.* **2005**, *95*, 205501.

[7] O. L. Krivanek, M. F. Chisholm, V. Nicolosi, T. J. Pennycook, G. J. Corbin, N. Dellby, M. F. Murfitt, C. S. Own, Z. S. Szilagyi, M. P. Oxley, S. T. Pantelides, S. J. Pennycook, *Nature* **2010**, *464*, 571–574.

[8] S. F. Pei, J. P. Zhao, J. H. Du, W. C. Ren, H. M. Cheng, *Carbon* **2010**, *48*, 4466–4474.

[9] a) W. Kohn, L. J. Sham, *Phys. Rev.* **1965**, *140*, A1133; b) P. E. Blöchl, *Phys. Rev. B* **1994**, *50*, 17953–17979; c) P. Hohenberg, W. Kohn, *Phys. Rev. B* **1964**, *136*, B864; d) G. Kresse, J. Furthmuller,

Phys. Rev. B **1996**, *54*, 11169 – 11186; e) G. Mills, H. Jonsson, *Phys. Rev. Lett.* **1994**, *72*, 1124 – 1127; f) J. P. Perdew, K. Burke, M. Ernzerhof, *Phys. Rev. Lett.* **1996**, *77*, 3865 – 3868.

[10] R. F. Egerton, *Electron Energy-loss Spectroscopy in the Electron Microscope*, 2ednd edPlenum, New York, **1996**.

[11] M. F. Chisholm, G. Duscher, W. Windl, *Nano Lett.* **2012**, *12*, 4651 – 4655.

[12] a) J. Kotakoski, J. C. Meyer, S. Kurasch, D. Santos-Cottin, U. Kaiser, A. V. Krasheninnikov, *Phys. Rev. B* **2011**, *83*, 245420; b) E. Cockayne, G. M. Rutter, N. P. Guisinger, J. N. Crain, P. N. First, J. A. Stroscio, *Phys. Rev. B* **2011**, *83*, 195425.

[13] A. Zobelli, A. Gloter, C. P. Ewels, G. Seifert, C. Colliex, *Phys. Rev. B* **2007**, *75*, 245402.

[14] C. J. Russo, J. A. Golovchenko, *Proc. Natl. Acad. Sci. USA* **2012**, *109*, 5953 – 5957.

[15] R. A. Serway, J. W. Jewett, *Physics for Scientists and Engineers*, Thomson-Brooks/Cole, **2004**.

[16] a) B. C. Stipe, M. A. Rezaei, W. Ho, *Science* **1998**, *279*, 1907 – 1909; b) H. L. Tierney, C. J. Murphy, A. D. Jewell, A. E. Baber, E. V. Iski, H. Y. Khodaverdian, A. F. McGuire, N. Klebanov, E. C. H. Sykes, *Nat. Nanotechnol.* **2011**, *6*, 625 – 629; c) U. G. E. Perera, F. Ample, H. Kersell, Y. Zhang, G. Vives, J. Echeverria, M. Grosolia, G. Rapenne, C. Joachim, S. W. Hla, *Nat. Nanotechnol.* **2013**, *8*, 46 – 51.

[17] J. Lee, W. Zhou, S. J. Pennycook, J. C. Idrobo, S. T. Pantelides, *Nat. Commun.* **2013**, *4*, 1650.

[18] a) M. Giovanni, H. L. Poh, A. Ambrosi, G. J. Zhao, Z. Sofer, F. Sanek, B. Khezri, R. D. Webster, M. Pumera, *Nanoscale* **2012**, *4*, 5002 – 5008; b) Y. Chen, X. C. Yang, Y. J. Liu, J. X. Zhao, Q. H. Cai, X. Z. Wang, *J. Mol. Graphics Modell.* **2013**, *39*, 126 – 132.